

Probing the Gas in Protoplanetary Disks with TEXES on Gemini-N

Joan R. Najita

The [Ne II] line at 12.81 microns has been suggested as a potential new probe of the planet formation region of circumstellar disks. It is a potentially powerful diagnostic because the neon in disks is expected to be fully in the gas phase and in atomic form. In addition, the 12.81-micron line probes warm, ionized gas, conditions which are believed to characterize the upper atmosphere of the inner disks surrounding classical T Tauri stars (Glassgold et al. 2007) and disk photoevaporative flows (Alexander 2008). Because it is sensitive to low column densities of gas, [Ne II] may also prove useful in identifying any residual gas surrounding weak-line T Tauri stars. Such measurements can potentially probe the dissipation timescale of gaseous disks and, thereby, constrain the timescale for giant planet formation.

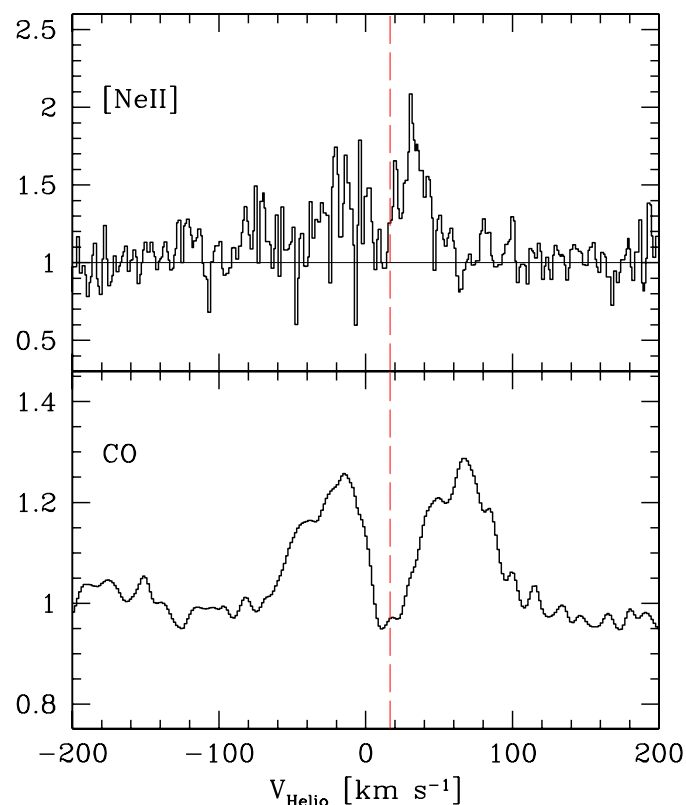


Figure 1: The 12.81-micron [Ne II] line profile (top) and the 4.9-micron CO line profile (bottom) of the T Tauri star AA Tau, both normalized to their respective continua. The vertical dashed line indicates the stellar velocity. The [Ne II] emission is centered near the stellar velocity, is broad (FWHM ~ 70 km/s), and is approximately double-peaked.

Observations with the Spitzer Space Telescope show that [Ne II] emission is, in fact, commonly detected from young stars, with line fluxes that are comparable to those predicted for disks (Glassgold et al. 2007). While the rough agreement between the predicted and

observed line fluxes is consistent with a disk origin for the emission, stronger confirmation for this interpretation can be obtained by measuring resolved [Ne II] line profiles.

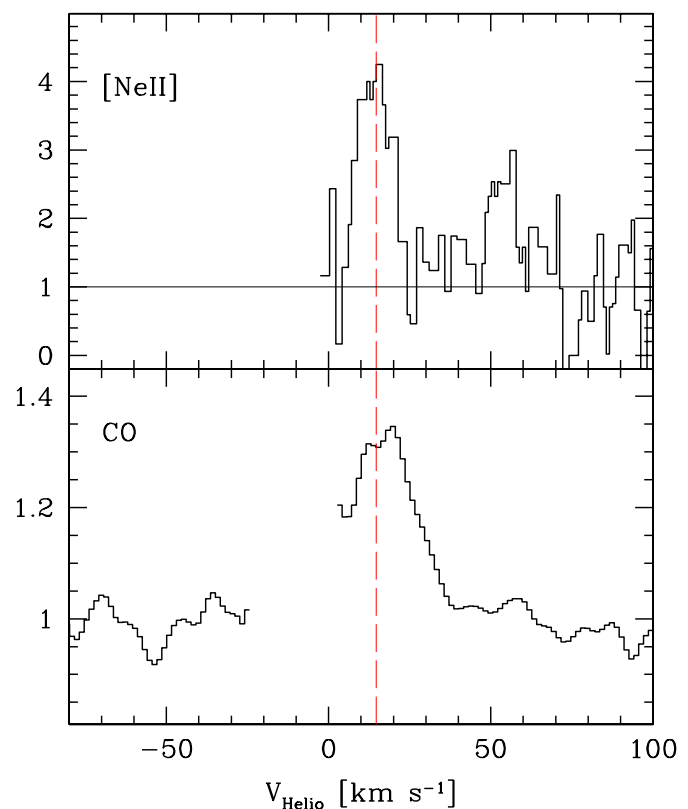


Figure 2: The 12.81-micron [Ne II] line profile (top) and the 4.7-micron CO line profile (bottom) of the T Tauri star GM Aur, both normalized to their respective continua. The vertical dashed line indicates the stellar velocity. The [Ne II] profile has a component of modest width (FWHM ~ 14 km/s) that is centered near the stellar velocity. There may be an additional emission component centered at ~ 40 km/s redward of the stellar velocity.

For that reason, we used the Texas Echelon Cross Echelle Spectrograph (TEXES) on Gemini North to study the [Ne II] line profiles of two young stars. TEXES is a sensitive, high resolution ($R \sim 80,000$) mid-infrared (5- to 25-micron) spectrometer. TEXES was offered at Gemini North as a visitor instrument in 2006B and again in 2007B, and our observations were carried out in 2007B. Our two targets, GM Aur and AA Tau, were known to show [Ne II] emission based on Spitzer spectroscopy and to have moderate to high system inclinations.

As reported in a paper recently accepted for the ApJ (Najita et al. 2009), we find that the [Ne II] emission from both sources is centered near the stellar velocity and is broader than the [Ne II] emission

continued

Probing the Gas in Protoplanetary Disks with TEXES continued

measured previously for the face-on disk system TW Hya (Herczeg et al. 2007). These properties are consistent with a disk origin for the emission we detect.

The increase in line width with increasing inclination strongly suggests that disk rotation (rather than photoevaporation or turbulence in a hot disk atmosphere) is primarily responsible for the line width. In the more highly inclined (non-face-on) systems that we studied, the [Ne II] emission is narrower than the CO fundamental emission from the same sources (see figures). If the widths of both diagnostics are dominated by Keplerian rotation, this suggests that the [Ne II] emission arises from larger disk radii on average than does the CO emission.

Interestingly, the equivalent width of the [Ne II] emission that we detected is less than that of the spectrally unresolved [Ne II] feature in the Spitzer spectra of the same sources. Variability in the [Ne II] emission or the mid-infrared continuum, a spatially extended [Ne II] component, or a very (spectrally) broad [Ne II] component might account for the difference.

Spatially extended [Ne II] emission is a distinct possibility. A recent study by van Boekel et al. (2009) using the Very Large Telescope

(VLT) spectrometer and imager for the mid-infrared (VISIR) shows that the [Ne II] emission from the T Tau triplet is spatially extended and associated with a known outflow in the system. Although the systems we studied do not show similar strong outflow activity, a weaker extended component may be present. While an extended component may be present, our observations, obtained with a 0.6-arcsec slit, show that the emission within ± 40 AU of the star likely has an origin in a gaseous disk, as expected theoretically.

These observations bring to a grand total of four the number of T Tauri [Ne II] emission sources that have been studied at high spectral resolution. Further measurements of resolved [Ne II] profiles are needed to determine whether the results obtained here apply to the majority of [Ne II]-emitting T Tauri stars. We therefore eagerly await a future opportunity to carry out such studies with TEXES on Gemini.

References:

Alexander, R.D. 2008, MNRAS, 391, L64
 Glassgold, A.E., Najita, J.R., & Igea, J. 2007, ApJ, 656, 515
 Herczeg, G.J., Najita, J.R., Hillenbrand, L.A., & Pascucci, I. 2007, ApJ, 670, 509
 Najita, J.R., et al. 2009, ApJ, 697, 957
 van Boekel, R., et al. 2009, A&A, 497, 137

NOAO 4-m Speckle Interferometry Observations of Massive Stars

Brian D. Mason & William I. Hartkopf (US Naval Observatory)

Massive stars appear to love company. Evidence continues to accumulate that the fraction of binary and multiple stars among the massive O- and B-type stars is much larger than that for solar type stars (see Zinnecker & Yorke 2007 and references therein). This difference in multiplicity properties may ultimately reflect differences in the star formation process between massive and low mass stars.

The observational evidence for the high incidence of binaries among the massive stars comes from both spectroscopic investigations of short-period systems and high angular resolution measurements of longer-period (and wide) binaries. Previous observations (Mason et al. 1998) made with the KPNO and CTIO 4-m telescopes and USNO speckle camera suggested that the true binary frequency may reach 100 percent among cluster stars, once account is made for the observational bias against detection of binaries with periods larger than those found spectroscopically but smaller than those found through high angular resolution measurements.

Ten years later (and armed with an improved detector) we decided it was an opportune time for follow up and expanded speckle observations. One system that was unobservable in the earlier effort, WR 146 (see figure 1), is now easily resolved into its constituent components. In Mason et al. (2009), we presented the results of this new speckle interferometric survey of Galactic massive stars, again made with the NOAO 4-m telescopes and USNO speckle camera, and sensitive to the detection of binaries in the angular separation regime between 0.03 arcsec and 5 arcsec with relatively bright companions $\Delta V < 3$). In this effort, new companions were first resolved for 14 OB stars. After combining our speckle data with published data on other visual companions detected through adaptive optics studies and/or noted in the Washington Double Star Catalog, as well as published information on radial velocities and spectroscopic binaries, a statistical analysis was made of the binary frequency among the subsample that are listed in the Galactic O Star Catalog (Maíz-Apellániz et al. 2007).

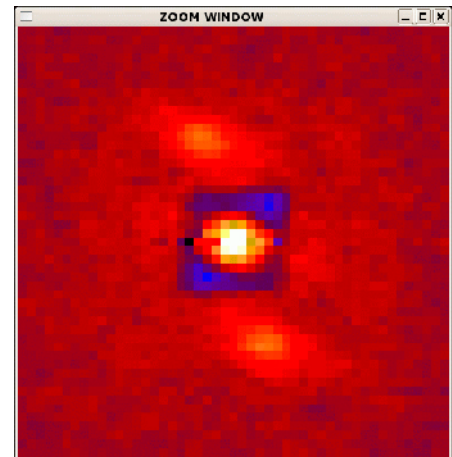


Figure 1: Directed vector autocorrelation of WR 146 = NML 1. The central peak is the zeroth order correlation while the near symmetric (due to the small Δm) peaks represent the primary and the secondary. Both components are fainter than 16th magnitude in V band, a challenge for speckle interferometry. First resolved in 1996 at 168 mas by Niemela et al. (1998), it had closed to 157 mas by the time of this observation and to 136 mas in 2008.

continued

NOAO 4-m Speckle Interferometry Observations continued

Table 1: Binary Frequency of Galactic O-Stars

Category	Cluster/ Association	Field	Runaway
A. Visual Multiplicity			
No. systems	249	56	42
$n = 2$	50	11	9
$n > 2$	58	3	2
Total	43%	25%	26%
$n = 1$	141	42	31
Total	57%	75%	74%
B. Spectroscopic Properties			
No. Stars	272	56	42
SB3O	7	0	0
SB2O	40	3	3
SB1O	14	0	5
SBE	5	3	0
SB2?	15	4	1
SB1?	45	8	3
Less SB?	30%	15%	19%
Total	57%	46%	29%
C	97	21	30
Total	43%	54%	71%
U	49	17	0
C. Fraction with Any Companion			
Less SB?	66%	41%	37%
Total	75%	59%	43%

Notes to table:

- SBn = spectroscopic binary (known or probable) with n companions
- O = has a published orbit
- E = exhibits eclipse or ellipsoidal light variations indicating a binary
- n? = suspected binary with line doubling ($n = 2$) or with radial velocity variations > 35 k/s ($n = 1$)
- C = constant velocity star
- U = unknown status

These binary statistics are summarized in table 1. We caution that the sample is magnitude limited (and therefore biased to more luminous stars) and incompletely surveyed (for example, the Turner et al., 2008 adaptive optics work is limited to stars with declination $> -42^\circ$). The stars are grouped into cluster/association, field, and runaway categories to compare their binary properties. For the immediate purpose of this work, we simply assigned any star that was not a field or runaway object to the cluster/association category. This includes stars described as more distant than some foreground cluster, since such stars generally reside along a spiral arm of the Galaxy, where cluster membership is common. The top section of table 1 summarizes the visual multiplicity properties of each category for the 347 unique, visual systems in the Galac-

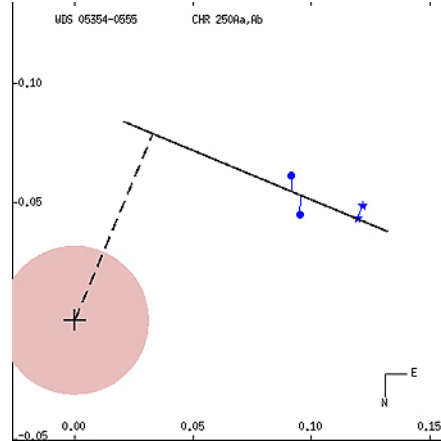


Figure 2: The relative motion of the components of i Ori = CHR 250. The straight line is a rectilinear fit to the four measures, indicating motion to the east-northeast. The shaded circle indicates the ~ 30 mas resolution limit of a 4-m telescope, while the dashed line indicates the closest separation of the two stars assuming their relative motion is rectilinear. The stars appear to have reached a closest separation of 82 ± 5 mas in 1969.7. Of course, the entire time span of observations of this pair is only about 11.5 years; we may instead be observing only a small arc of a long-period orbit.

tic O Star Catalog. The results are presented in rows that correspond to the sum based upon the number of visual components n found. We divide the sample into single and multiple groups in determining the percentages with and without companions (making the tacit assumption that most of the visual companions are gravitationally bound and not line-of-sight optical companions).

The middle section of table 1 presents the corresponding sums for the spectroscopic binary properties for all 370 entries in the Galactic O Star Catalog. The percentages for each subgroup represent fractions with the unknown “U” status objects excluded from the totals. Finally, the lower section in table 1 shows the percentages for the presence of any companion (spectroscopic or visual) again excluding the stars with unknown spectroscopic status.

In addition to the study of the population multiplicity characteristics, detailed analysis was possible for some specific systems:

i Ori: The complex dynamical relationship of AE Aur, μ Col, and i Ori is one of the best examples of a binary-binary collision

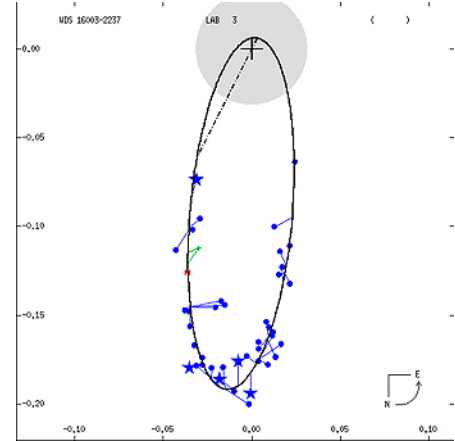


Figure 3: New orbit for δ Sco = LAB 3. The figure shows the relative motion of the secondary about the primary (indicated by a large “plus” sign); the x and y scales are in arcseconds. The solid curve represents the new orbit determination. The dot-dash line indicates the line of nodes. New measures are shown as filled stars and all other high resolution measurements as filled circles. Micrometer measures are indicated by small plus signs, the Hipparcos measure by a red “H.” All measurements are connected to their predicted positions on the orbit by “O – C” lines. The north-east orientation of the orbit and the direction of motion are indicated in the lower right corner of the plot. The gray filled circle centered on the primary represents that region where the pair is too close to be resolved by speckle interferometry with a 4-m telescope.

(Gies & Bolton 1986). As i Ori is a known close pair ($P = 29.13376$ d; Marchenko et al. 2000), the much wider speckle component would be hierarchical if physical, with an estimated period of at least 40 y (Gualandris et al. 2004). As the high energy needed to eject AE Aur and μ Col with their runaway velocities seemed inconsistent with the less energetic dynamical interaction required for the CHR 250 pair (i Ori) to remain bound, Gualandris et al. postulated that this pair was non-physical, despite their close proximity. Figure 2 shows a weighted least-squares, linear fit to the published data. It is worth noting that the data are also consistent with a long-period orbit, but one much longer than 40 y.

δ Sco: Bedding (1993) published the first set of orbital elements for δ Sco based solely on interferometric data. Miroschnichenko et al. (2001) obtained complementary radial velocity data that tied down T quite precisely and also gave a more accurate estimate of

continued

NOAO 4-m Speckle Interferometry Observations continued

the eccentricity, while adopting the values for period and semi-major axis obtained by Hartkopf et al. (1996). Since the 1996 solution, observations have covered over one additional revolution. A new orbital solution (figure 3) was determined, utilizing all available interferometric data and adopting the *T* and eccentricity values of Miroschnichenko et al. (2001).

References:

Bedding, T. 1993, *AJ*, 206, 768
 Gies, D.R., & Bolton, C.T. 1986, *ApJS*, 61, 419
 Gualandris, A., et al. 2004, *MNRAS*, 350, 615
 Hartkopf, W.I., Mason, B.D., & McAlister, H.A. 1996, *AJ*, 111, 370
 Maíz-Apellániz, J., et al. 2007, *ApJ*, 660, 1480
 Marchenko, S.V., et al. 2000, *MNRAS*, 317, 333
 Mason, B.D., et al. 1998, *AJ*, 115, 821
 Mason, B.D., et al. 2009, *AJ*, 137, 3358
 Miroschnichenko, A.S., et al. 2001, *A&A*, 377, 485
 Niemela, V.S., et al. 1998, *AJ*, 115, 2047
 Turner, N.H., et al. 2008, *AJ*, 136, 554
 Zinnecker, H., & Yorke, H.W. 2007, *ARA&A*, 45, 481

Comparing Magnetic Fields in the Solar Photosphere and Chromosphere at Equatorial and Polar Latitudes

Gordon Petrie (NSO) & Irina Patrikeeva (Northwestern University; 2008 NSO REU Student)

The Synoptic Optical Long-term Investigations of the Sun (SOLIS) Vector Spectromagnetograph (VSM) is unique, producing full-disk line-of-sight (LOS) magnetograms of the solar photosphere and chromosphere. It has done so daily since August 2003. Figure 1 shows a photospheric image (left) and a chromospheric image (right) from the same day. Light grey denotes positive magnetic field (outward from the Sun), and dark grey denotes negative field. These images are little more than an hour apart and their similarity is clear. Yet there are subtle differences: magnetic features appear slightly larger and are more diffuse in the chromosphere than in the photosphere. Furthermore, features close to the limb appear stronger in the chromosphere than in the photosphere.

The magnetic field of the solar corona is the cause of the most spectacular events in the heliosphere. Since the coronal field is very difficult to measure, global atmospheric field models and solar wind predictions are usually based on extrapolations from measurements of the photospheric field. While physical conditions in the chromosphere are closer to coronal conditions, chromospheric data have not been widely used because of their relative scarcity.

Global atmospheric field models can apply as boundary conditions on the magnetic field component along either the radial direction or the observer's LOS. Initially, the LOS component was routinely used in practice. This approach relies on the model description being valid

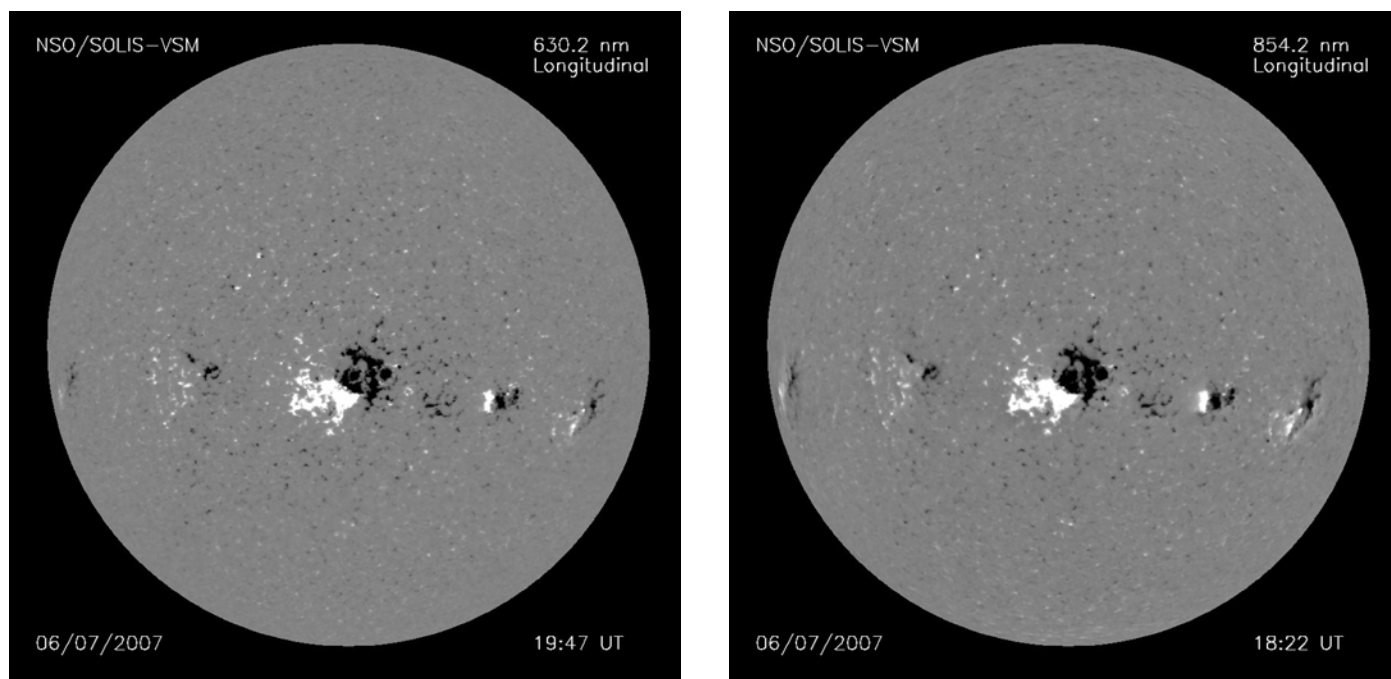


Figure 1: Full-disk, line-of-sight magnetograms of the solar photosphere (left) and chromosphere (right) taken approximately one hour apart.

continued

Comparing Magnetic Fields continued

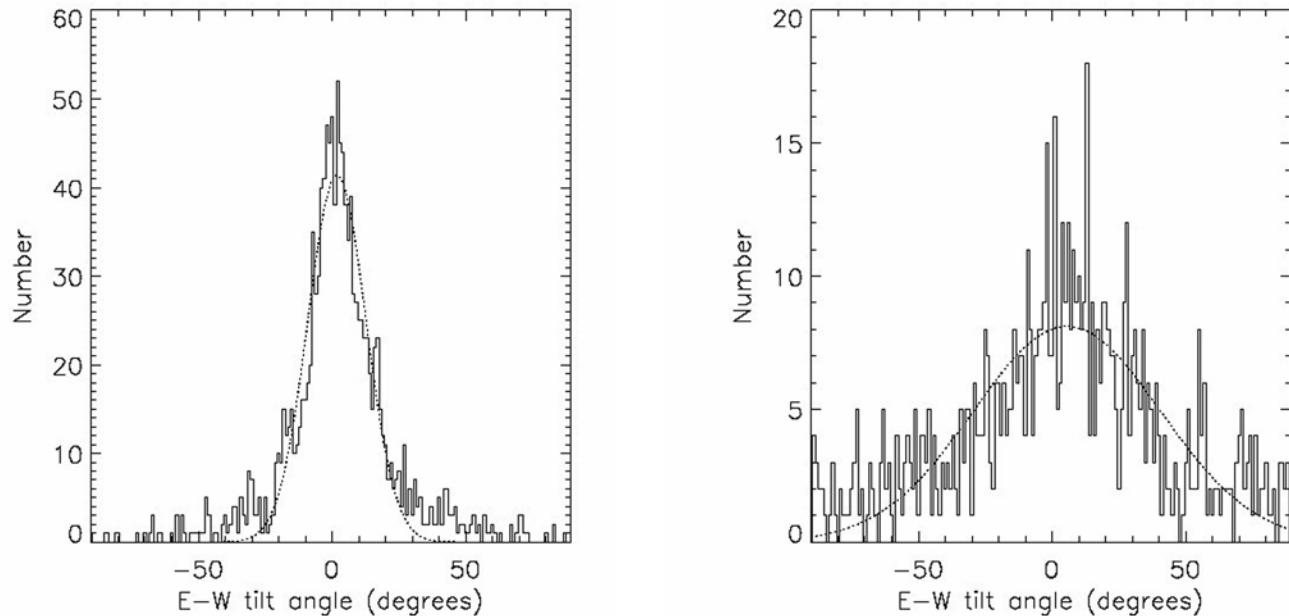


Figure 2. East–West tilt angles of low-latitude photospheric (left) and chromospheric (right) fields based on ≈3000 magnetograms.

throughout the atmosphere, whereas conditions in the photosphere and corona differ greatly as far as forces and currents are concerned. Moreover, because of projection effects, nearly radial fields close to the poles are barely represented in LOS boundary conditions and are not well reproduced in the model. Some years ago, it was found that more successful models are produced if the boundary conditions are derived based on the assumption that the photospheric field is radial. In such models, the photospheric measurements are separated from the approximately force-free, current-free corona by a thin current layer that idealizes the transition region. This approach also naturally produces an enhanced polar field and, in practice, the calculated models are in much improved agreement with observations. Despite this success, the photospheric radial field assumption is often criticized because non-radial fields are often found in measurements, particularly in active regions, e.g., see the recently released vector field measurements from the VSM. Furthermore, Harvey et al. (2007) discovered a dynamic horizontal component of the photospheric field of the quiet Sun using GONG and SOLIS LOS data (see June 2007 *Newsletter*).

We obtained estimates of the East–West tilt angles of low-latitude photospheric and chromospheric fields based on around 3000 magnetograms. We rejected cases where fields were not characterized by a well-defined direction throughout their disk passage. Some fields evolved significantly during their disk passage, and some field structure was complex and did not have a prevalent field direction. In most cases, however, a good vector fit was obtained. The photospheric and chromospheric distributions of these East–West tilt angles are shown in figure 2. The photospheric histogram is clearly more peaked than the chromospheric one. The best-fitting Gaussians to the histograms had maxima at 1.8° and 5.5° and half-widths at 10.8° and 35°. We concluded that the magnetic fields in the solar photosphere and the chromosphere behave distinctly differently. Most of the photospheric field is nearly radial, while the chromospheric field is more complex and has no strongly preferred direction, expanding

in all directions to a significant degree in a manner consistent with a canopy-like configuration.

A further issue is the sensitivity of the models to the fields that are most poorly observed of all: the polar fields. The two magnetic polar caps are large-scale flux distributions each dominated by a single polarity. However, the LOS field signal derived from photospheric line polarization is not strong enough to allow accurate information on the flux distribution near the poles. In models, the global large-scale structure is unfortunately dominated by the polar dipole component, which is particularly sensitive to boundary conditions for the polar fields. The sensitivity of the VSM and the high spatial resolution of the images allow us to sample the fields with better spatial resolution than has been possible in the past. The use of a chromospheric line allows us to estimate the polar field at chromospheric heights for the first time.

We did this not via forward models as in past studies, but by inverting the stereoscopic projections of the field vector at a given latitude along different lines of sight at different times of the year. The analysis revealed poleward monotonic increases in intensity and domination by a single polarity. The photospheric polar field structure was approximately steady between 2003 and 2008, while the chromospheric field appears to have been more time-varying, becoming approximately steady only approaching activity minimum in 2008. We found that the photospheric field was approximately radial in both polar caps between 2003 and 2008 and had peaked field intensity distribution, increasing poleward, and varying approximately as $B_{\text{pole}} \cos^n \theta$ with $B_{\text{pole}} = -5.3$ and $n = 8.8$ at the North pole, and $B_{\text{pole}} = 5.8$ and $n = 9.7$ at the South pole, where θ is the co-latitude. The chromospheric field tended to expand super-radially in the South during 2008.

A complete discussion on this topic has been accepted for publication in the *Astrophysical Journal*. 